

# Ballistic SNS sandwich as a $\pi$ Josephson junction

Edouard B. Sonin\*

Racah Institute of Physics, Hebrew University of Jerusalem, Givat Ram, Jerusalem 9190401, Israel

(Dated: May 18, 2022)

The paper develops the theory of the ballistic SNS sandwich, in which the Josephson effect exists without the proximity effect. The analysis essentially revised the conclusions of previous works. The ballistic SNS sandwich is a  $\pi$  Josephson junction because its ground state corresponds not to zero Josephson phase but to the phases  $\pm\pi$ . The analysis does not confirm previous predictions on strong suppression of the supercurrent at temperatures on the order or higher than the energy distance between Andreev levels. The disagreement is explained by violations of the charge conservation in the previous investigations. Other unusual properties of the ballistic SNS sandwich are also discussed: the absence of the Josephson plasma mode localized at the normal layer, the Meissner effect, and the Josephson vortex structure.

## I. INTRODUCTION

Originally the Josephson junction was considered as an insulator or normal metal bridge between two superconductors. The Josephson coupling between superconductors was provided due to penetration of the superconducting order parameter into the bridge (proximity effect) if the bridge is not too long compared with the coherence length. However, it was noticed long ago [1–3] that if the bridge is a ballistic normal metal the Josephson coupling is possible even for rather long bridges. This was demonstrated in an idealized model of the ballistic SNS sandwich (planar SNS Josephson junction). There is a normal layer of width  $L$  between two superconductors. The layers are perpendicular to the axis  $x$  (Fig. 1). The effective masses and Fermi energies are the same in the superconductors and in the normal metal; the only difference is that the pair potential sharply vanishes in the normal layer  $-L/2 < x < L/2$ . Investigations of this model continue up to now [4]. The ballistic SNS Josephson junction was studied for unconventional pairing in high- $T_c$  superconductors [5]. There were theoretical and experimental investigations for other materials bridging two superconductors: graphene [6, 7], topological insulator [8], and nanotubes [9].

Previous theoretical investigations of the ballistic SNS sandwich have left some questions unanswered up to now. Ishii [2] noticed that canonical relations for the pair of Hamiltonian conjugated variables “charge–phase” were not satisfied. There was a problem with the charge conservation law because the theory postulated some spatial distribution of the order parameter (gap) without solving the self-consistency equation for gap, which determines this distribution. There were also disagreements on the final form of the current–phase relation.

The present paper suggests an approach free of those flaws. This led to a serious revision of previous results. It was demonstrated that in the ground state of the SNS sandwich the phase difference across the junction is not

zero but  $\pm\pi$ . Therefore, the SNS sandwich is a so-called  $\pi$  junction. In the past  $\pi$  junctions were predicted and observed in ferromagnetic junctions [10], junctions with unconventional superconductivity [11], nanotube junctions [9], quantum dot junctions [12], and SINIS junctions [13]. Our analysis demonstrates the existence of a SNS  $\pi$  junction without ferromagnetism and for  $s$ -wave superconductivity.

Another important outcome of our analysis is the absence of strong suppression of the supercurrent at temperatures comparable with the energy distance between Andreev levels, which was predicted in previous investigations [1–3]. Since the energy distance between Andreev levels is usually much smaller than the critical temperature for superconductivity, this promises to make exper-

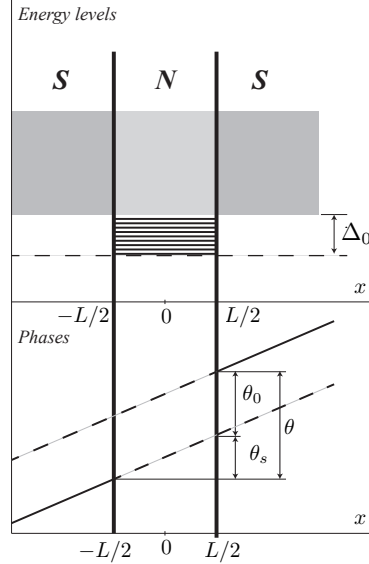


FIG. 1. Energy levels and phases in the SNS sandwich. The interval of continuum states is shaded. The Andreev bound states inside the gap  $\Delta_0$  are shown by solid lines. The lower part of the figure shows the bound-state phase  $\theta_0$ , the superfluid phase  $\theta_s$ , and the Josephson phase  $\theta$ .

\* sonin@cc.huji.ac.il

imental detection of the supercurrent easier.

The ballistic SNS junction is not a weak link, and therefore, there is no Josephson plasma mode with the frequency much lower than the plasma frequency in the superconducting layer and no suppression of the Meissner effect in the normal layer. A weak magnetic field penetrates into the normal layer on the same London penetration depth as into the superconducting layers, in contrast to usual Josephson junctions with the Josephson penetration depth much larger than the London penetration depth. At stronger magnetic fields the Josephson vortices appear with the core size of the order of the normal layer thickness  $L$ . Since their energy is lower than the energy of bulk Abrikosov vortices, Josephson vortices are pinned to the normal layer, and the first critical magnetic field for the SNS junction is smaller than that for superconducting bulk, but not so small as in usual Josephson junctions.

The analysis mostly addresses the 1D case. Its generalization on the 2D and 3D cases is straightforward. Integration over spaces of transverse wave vectors in 2D and 3D cases results in replacement of the 1D electron density by 2D and 3D densities respectively in all expressions for currents, which become current densities.

## II. THE BOGOLYUBOV-DE GENNES THEORY

Since in our model the order parameter  $\Delta$  is supposed to be known we do not need the full BCS Hamiltonian with the interaction term quartic in the electron wave function. It is sufficient to use the quadratic in the wave function second-quantized effective Hamiltonian introduced in the self-consistent field method [14]. Its density is

$$\mathcal{H}_{eff} = \frac{\hbar^2}{2m} [\nabla \hat{\psi}_\alpha^\dagger(x) \nabla \hat{\psi}_\alpha(x) - k_f^2 \hat{\psi}_\alpha^\dagger(x) \hat{\psi}_\alpha(x)] + \Delta \hat{\psi}_\uparrow^\dagger(x) \hat{\psi}_\uparrow(x) + \Delta^* \hat{\psi}_\downarrow(x) \hat{\psi}_\uparrow(x), \quad (1)$$

where  $\hat{\psi}_\alpha^\dagger(x)$  and  $\hat{\psi}_\alpha(x)$  are operators of creation and annihilation of an electron, and the subscript  $\alpha$  has two values corresponding to the spin up ( $\uparrow$ ) and down ( $\downarrow$ ). We address a 1D problem with the Fermi wave number  $k_f$ , assuming that our system is uniform in the plane normal to the axis  $x$ . In multidimensional (2D and 3D) systems with the Fermi wave number  $k_F$   $k_f = \sqrt{k_F^2 - k_\perp^2}$ , where  $k_\perp$  is the transverse component of the multidimensional wave vector  $\mathbf{k}$ . The complex order parameter, or gap,  $\Delta$  can vary in space and time.

The quadratic effective Hamiltonian can be diagonalized by the Bogolyubov-Valatin transformation from the free electron operators  $\hat{\psi}_\alpha^\dagger(x)$  and  $\hat{\psi}_\alpha(x)$  to the quasiparticle operators  $\hat{a}_{i\alpha}^\dagger$  and  $\hat{a}_{i\alpha}$

$$\hat{\psi}_\uparrow(x) = \sum_i \left[ u_i(x) \hat{a}_{i\uparrow} - v_i^*(x) \hat{a}_{i\downarrow}^\dagger \right],$$

$$\hat{\psi}_\downarrow(x) = \sum_i \left[ u_i(x) \hat{a}_{i\downarrow} + v_i^*(x) \hat{a}_{i\uparrow}^\dagger \right]. \quad (2)$$

For the diagonalization of effective Hamiltonian the functions  $u_i(x)$  and  $v_i(x)$  must be stationary solutions of the time-dependent Bogolyubov-de Gennes equations [15]:

$$\begin{aligned} i\hbar \frac{\partial u}{\partial t} &= \frac{\delta \mathcal{H}}{\delta u^*} = -\frac{\hbar^2}{2m} (\nabla^2 + k_f^2) u + \Delta v, \\ i\hbar \frac{\partial v}{\partial t} &= \frac{\delta \mathcal{H}}{\delta v^*} = \frac{\hbar^2}{2m} (\nabla^2 + k_f^2) v + \Delta^* u. \end{aligned} \quad (3)$$

The summation over the subscript  $i$  means the summation over all bound and continuum states corresponding to stationary solutions of the Bogolyubov-de Gennes equations Eq. (3). The Bogolyubov-de Gennes equations are the Hamilton equations with the Hamiltonian (per unit volume)

$$\begin{aligned} \mathcal{H}_{BG} = \frac{\hbar^2}{2m} (|\nabla u|^2 - k_f^2 |u|^2) - \frac{\hbar^2}{2m} (|\nabla v|^2 - k_f^2 |v|^2) \\ + \Delta u^* v + \Delta^* v^* u. \end{aligned} \quad (4)$$

After the diagonalization the effective Hamiltonian becomes

$$\mathcal{H}_{eff} = \sum_i \varepsilon_i (a_{i\uparrow}^\dagger a_{i\uparrow} + a_{i\downarrow}^\dagger a_{i\downarrow} - 2|v|^2), \quad (5)$$

where  $\varepsilon_i$  is the energy of the  $i$ the quasiparticle state.

In general the functions  $u(x, t)$  and  $v(x, t)$  can be considered as two components of a spinor wave function,

$$\psi(x, t) = \begin{pmatrix} u(x, t) \\ v(x, t) \end{pmatrix}, \quad (6)$$

describing a state of a quasiparticle, which is a superposition of a state with one particle (upper component  $u$ ) and a state with one antiparticle, or hole (lower component  $v$ ). The number of particles (charge) is not a quantum number of the state.

The Hamiltonians Eq. (1) and Eq. (4) are not gauge-invariant, and therefore the total number of electrons (charge) is not a conserved quantity. The continuity equation for the electron fluid is

$$\frac{\partial n}{\partial t} + \frac{1}{e} \nabla j = \frac{2i}{\hbar} (\Delta^* v^* u - \Delta v u^*), \quad (7)$$

where

$$n = |u|^2 - |v|^2 \quad (8)$$

is the electron density, and

$$j = -\frac{ie\hbar}{2m} (u^* \nabla u - u \nabla u^*) - \frac{ie\hbar}{2m} (v^* \nabla v - v \nabla v^*) \quad (9)$$

is the electric current. The charge conservation law restores if one solves the Bogolyubov-de Gennes equations Eq. (3) together with the self-consistency equation. However, we adopt the approach used earlier [1-3]. Instead of

solving the self-consistency equation we simply postulate the gap  $\Delta$  of constant modulus  $\Delta_0 = |\Delta|$  in the superconducting layers and zero gap inside the normal layer. The model is expected to be valid if the thickness  $L$  of the normal layer essentially exceeds the coherence length

$$\zeta_0 = \frac{\hbar v_f}{\Delta_0}. \quad (10)$$

Although in the Bogolyubov-de Gennes theory the charge is not conserved, there is another important conservation law for the total number of quasiparticles. The continuity equation for them is

$$\frac{\partial \mathcal{N}}{\partial t} + \nabla g = 0, \quad (11)$$

where

$$\mathcal{N} = |u|^2 + |v|^2 \quad (12)$$

is the quasiparticle density, and

$$g = -\frac{i\hbar}{2m}(u^* \nabla u - u \nabla u^*) + \frac{ie\hbar}{2m}(v^* \nabla v - v \nabla v^*) \quad (13)$$

is the current, which will be called the quasiparticle flux. While the density  $n$  is the difference of the densities of particles and holes, the density  $\mathcal{N}$  is the sum of these two densities.

The density  $n$  and the charge current  $j$  in equations above are expectation values for the operators

$$\begin{aligned} \hat{n}(x) &= \hat{\psi}_\uparrow^\dagger(x)\hat{\psi}_\uparrow(x) + \hat{\psi}_\downarrow^\dagger(x)\hat{\psi}_\downarrow(x) \\ &= \sum_i \left[ |u_i(x)|^2 \hat{a}_{i\uparrow}^\dagger \hat{a}_{i\uparrow} + |v_i(x)|^2 \hat{a}_{i\downarrow}^\dagger \hat{a}_{i\downarrow} \right] \\ &= \sum_i \left[ |u_i(x)|^2 \hat{a}_{i\uparrow}^\dagger \hat{a}_{i\uparrow} - |v_i(x)|^2 \hat{a}_{i\downarrow}^\dagger \hat{a}_{i\downarrow} + 2|v_i(x)|^2 \right] \quad (14) \\ \hat{j} &= -\frac{ie\hbar}{2m} \sum_i \left[ (u_i^* \nabla u_i - u_i \nabla u_i^*) \hat{a}_{i\uparrow}^\dagger \hat{a}_{i\uparrow} \right. \\ &\quad \left. + (v_i^* \nabla v_i - v_i \nabla v_i^*) \hat{a}_{i\downarrow}^\dagger \hat{a}_{i\downarrow} - 2(v_i^* \nabla v_i - v_i \nabla v_i^*) \right]. \quad (15) \end{aligned}$$

There are similar expressions for  $\hat{\mathcal{N}}$  and  $\hat{g}$  in Eqs. (12) and (13).

There are two additive contributions to the total values of the density and the current. One is the vacuum contribution calculated assuming that all energy levels are not occupied (quasiparticle vacuum). This is given by last terms in Eqs. (14) and (15), which do not contain any quasiparticle operator. The other terms in Eqs. (14) and (15) yield the quasiparticle (excitation) contribution due to possible occupation of energy levels.

In a resting uniform superconductor with the constant  $\Delta_0$  solutions of the Bogolyubov-de Gennes equations are plane waves

$$\begin{pmatrix} u_0 \\ v_0 \end{pmatrix} e^{ik \cdot x - i\varepsilon_0 t / \hbar}, \quad (16)$$

where

$$u_0 = \sqrt{\frac{1}{2} \left( 1 + \frac{\xi}{\varepsilon_0} \right)}, \quad v_0 = \sqrt{\frac{1}{2} \left( 1 - \frac{\xi}{\varepsilon_0} \right)}. \quad (17)$$

The quasiparticle energy is given by the well known BCS expression

$$\varepsilon_0 = \sqrt{\xi^2 + \Delta_0^2}. \quad (18)$$

Here  $\xi = (\hbar^2/2m)(k^2 - k_f^2) \approx \hbar v_f (k - k_f)$  is the quasiparticle energy in the normal Fermi liquid, and  $v_f = \hbar k_f / m$  is the Fermi velocity. The states with positive and the negative signs of  $\xi$  correspond to particle-like and the hole-like branches of the spectrum respectively. Note that mathematically the Bogolyubov-de Gennes equations have solutions with negative and positive energies  $\pm \varepsilon_0$ . But only solutions with positive energy  $\varepsilon_0$  have the physical meaning [16]. In fact, taking into account solutions with negative energy would be a double-counting since hole-like solutions with positive energy but with  $k < k_f$  (negative  $\xi$ ) have represent all states inside the Fermi surface.

### III. BOUND ANDREEV AND CONTINUUM STATES

#### A. Andreev bound states

The spectrum and the wave function for the present model of the SNS sandwich have been already investigated in previous works, and it is sufficient here to present the resume of these investigations. In the limit of large Fermi wave numbers  $k_f \gg \Delta_0 / \hbar v_f$  the Bogolyubov-de Gennes equations of the second order in gradients are reduced to the equations of the first order. As a result, the boundary conditions on the interfaces between the normal and superconducting layers require the continuity of the wave function components  $u$  and  $v$  but not their gradients. The components  $u$  and  $v$  are superpositions of plane waves with wave numbers close to either only  $+k_f$ , or only  $-k_f$ . This means that at interfaces between normal and superconducting layers only Andreev reflection is possible, which does not change the quasiparticle momentum essentially, but the quasiparticle group velocity changes its sign.

Because of Andreev reflection, there are Andreev bound states with energies  $\varepsilon_0 < \Delta_0$  localized in the normal layer. The wave functions of these states, which satisfy the Bogolyubov-de Gennes equations and the boundary conditions, are given by

$$\begin{pmatrix} u \\ v \end{pmatrix} = \sqrt{\frac{N}{2}} \begin{pmatrix} e^{\pm \frac{i\eta}{2} \pm \frac{im\varepsilon_0}{\hbar^2 k_f} (x - L/2)} \\ e^{-i\theta_{\pm} \mp \frac{i\eta}{2} \mp \frac{im\varepsilon_0}{\hbar^2 k_f} (x - L/2)} \end{pmatrix} e^{\pm ik_f \cdot x} \quad (19)$$

inside the normal layer  $-L/2 < x < L/2$ ,

$$\begin{pmatrix} u \\ v \end{pmatrix} = \sqrt{\frac{N}{2}} \begin{pmatrix} e^{\pm \frac{i\eta}{2}} \\ e^{-i\theta_+ \mp \frac{i\eta}{2}} \end{pmatrix} e^{\pm ik_f x - (x - L/2)/\zeta} \quad (20)$$

inside the superconducting layer at  $x > L/2$ , and

$$\begin{pmatrix} u \\ v \end{pmatrix} = \sqrt{\frac{N}{2}} \begin{pmatrix} e^{\mp \frac{i\eta}{2}} \\ e^{-i\theta_- \pm \frac{i\eta}{2}} \end{pmatrix} e^{\pm ik_f x + (x + L/2)/\zeta} \quad (21)$$

inside the superconducting layer at  $x < -L/2$ . Here

$$e^{i\eta} = \frac{\varepsilon_0 + i\sqrt{\Delta_0^2 - \varepsilon_0^2}}{\Delta_0}, \quad \cos \eta = \frac{\varepsilon_0}{\Delta_0}, \quad \sin \eta = \frac{\sqrt{\Delta_0^2 - \varepsilon_0^2}}{\Delta_0} \quad (22)$$

and  $\theta_+$  and  $\theta_-$  are the order parameter phases at  $x = L/2$  and  $x = -L/2$  respectively. The upper and lower signs correspond to the wave number semi-spaces  $k > 0$  and  $k < 0$  respectively. The normalization constant

$$N = \frac{1}{L + \zeta} \quad (23)$$

takes into account the penetration of the bound states into the superconducting layers with the penetration depth

$$\zeta = \zeta_0 \frac{\Delta_0}{\sqrt{\Delta_0^2 - \varepsilon_0^2}}, \quad (24)$$

which diverges when  $\varepsilon_0$  approaches to the gap  $\Delta_0$ .

The boundary conditions are satisfied at the Bohr-Sommerfeld condition,

$$\varepsilon_0(s, \pm\theta_0) = \frac{\hbar v_f}{2L} (2\pi s + 2\eta \pm \theta_0), \quad (25)$$

which determines the energies of the Andreev states. Here  $\theta_0 = \theta_+ - \theta_-$  and  $s$  is an arbitrary integer. The notation  $s$  for integers will appear further also in other expressions, although its value would be chosen differently. The two signs before  $\theta_0$  correspond to positive and negative signs of the 1D wave numbers in the Andreev states. Further we shall call the phase difference  $\theta_0$  across the normal layer the bound-state phase, because it shifts the bound states with respect to the gap.

Equation (25) is not an expression but an equation for  $\varepsilon_0$ , since according to Eq. (22)  $\eta$  depends on  $\varepsilon_0$ . At small energy  $\varepsilon_0 \ll \Delta_0$ ,  $\eta = \pi/2$ , and the spectrum of the bound states is

$$\varepsilon_0 = \frac{\hbar v_f}{2L} \left[ 2\pi \left( s + \frac{1}{2} \right) \pm \theta_0 \right]. \quad (26)$$

At the energy  $\varepsilon_0$  close to  $\Delta_0$  ( $\Delta_0 - \varepsilon_0 \ll \Delta_0$ ) one can use the approximation

$$\eta \approx 2\pi s + \sqrt{\frac{2(\Delta_0 - \varepsilon_0)}{\Delta_0}}. \quad (27)$$

Then solution of Eq. (25) for  $\varepsilon_0$  yields

$$\varepsilon_0 = \Delta_0 - \frac{\hbar^2 v_f^2}{2\Delta_0 L^2} \left\{ \sqrt{1 + \frac{\Delta_0 L}{\hbar v_f} [2\pi(s + \alpha) \mp \theta_0]} - 1 \right\}^2, \quad (28)$$

where  $\alpha$  is the fractional part of the ratio

$$\frac{\Delta_0 L}{\pi \hbar v_f} = s + \alpha. \quad (29)$$

An integer  $s$  is chosen so that  $0 < \alpha < 1$ . The parameter  $\alpha$  is the measure of incommensurability of the gap  $\Delta_0$  with the interlevel energy distance.

In any  $s$ -th Andreev state there is a charge current determined by the canonical relation

$$j(s) = \frac{2e}{\hbar} \frac{\partial \varepsilon_0}{\partial \theta_0} = \pm \frac{ev_f}{L + \zeta}. \quad (30)$$

The factor 2 takes into account that  $\theta_0$  is the phase of a Cooper pair but not of a single electron. As expected, this expression fully agrees with the fact that the mass current is the total momentum  $\hbar k_f$  in the state divided by the size  $L + \zeta$  of the bound state.

The existence of charge current in a bound state is the consequence of the absence of the charge conservation law in our model. At the same time, the quasiparticle flux given by Eq. (13) vanishes in accordance with the conservation law Eq. (11) for the total number of quasiparticles.

## B. Continuum states

Delocalized continuum states with  $\varepsilon_0 > \Delta_0$  are scattering states. For a quasiparticle ( $\xi > 0$ ) incident from left and propagating from  $x = -\infty$  to  $x = \infty$  the wave function is

$$\begin{pmatrix} u_0(\xi) \\ v_0(\xi) e^{-i\theta_-} \end{pmatrix} e^{i \left( k_f + \frac{m\xi}{\hbar^2 k_f} \right) x} + r \begin{pmatrix} u_0(-\xi) \\ v_0(-\xi) e^{-i\theta_-} \end{pmatrix} e^{i \left( k_f - \frac{m\xi}{\hbar^2 k_f} \right) x} \quad (31)$$

for  $x < -L/2$ , and

$$t \begin{pmatrix} u_0(\xi) \\ v_0(\xi) e^{-i\theta_+} \end{pmatrix} e^{i \left( k_f + \frac{m\xi}{\hbar^2 k_f} \right) x} \quad (32)$$

for  $x > L/2$ . Here  $t$  and  $r$  are amplitudes of transmission and reflection ( $|t|^2 + |r|^2 = 1$ ), which are determined from the continuity of spinor components at  $x = \pm L/2$  [3]. As in the case of bound states, the analysis considers only the Andreev reflection. The reflection and the transmission probabilities are

$$R(\theta_0) = |r|^2 = \frac{\Delta_0^2 \left[ 1 - \cos \left( \frac{2\varepsilon_0 m L}{\hbar^2 k_f} - \theta_0 \right) \right]}{2\varepsilon_0^2 - \Delta_0^2 - \Delta_0^2 \cos \left( \frac{2\varepsilon_0 m L}{\hbar^2 k_f} - \theta_0 \right)}, \quad (33)$$

$$\mathcal{T}(\theta_0) = |t|^2 = \frac{2(\varepsilon_0^2 - \Delta_0^2)}{2\varepsilon_0^2 - \Delta_0^2 - \Delta_0^2 \cos\left(\frac{2\varepsilon_0 m L}{\hbar^2 k_f} - \theta_0\right)}. \quad (34)$$

The spinor in the normal layer  $-L/2 < z < L/2$  is given by the same expression as Eq. (19) for the bound state, but with different normalization constant  $N = \mathcal{T}$ .

Similar expressions with the same  $R(\theta_0)$  and  $\mathcal{T}(\theta_0)$  can be derived for holes incident from right and moving to left. For a quasiparticle incident from right and a hole incident from left the reflection and the transmission probabilities are  $R(-\theta_0)$  and  $\mathcal{T}(-\theta_0)$ .

The transmission probability differs from unity in the energy interval of the order  $\Delta_0$  small with respect to the Fermi energy  $\varepsilon_f = \hbar^2 k_f^2 / 2m$ . The condition  $R + \mathcal{T} = 1$  follows from the conservation law for the number of quasiparticles, which leads to the constant quasiparticle flux  $g$  in the whole space [see Eq. (13)]. The scattering delocalized states in the SNS sandwich were determined for  $\theta_0 = 0$  by Bardeen and Johnson [3] and for  $\theta_0 \neq 0$  in Refs. 17 and 18.

One can transform expressions for  $R$  and  $\mathcal{T}$  demonstrating their dependence on the incommensurability parameter  $\alpha$ . Taking into account Eq. (29), the transmission probability is

$$\mathcal{T} = \frac{2(\varepsilon_0^2 - \Delta_0^2)}{2\varepsilon_0^2 - \Delta_0^2 - \Delta_0^2 \cos\left[\frac{2(\varepsilon_0 - \Delta_0)mL}{\hbar^2 k_f} + 2\pi\alpha - \theta_0\right]}. \quad (35)$$

The reflection probability can be transformed similarly. The both probabilities have fast oscillating parts periodical in  $2\pi\alpha - \theta_0$ . For the further analysis mostly the probability averaged over these oscillations is important:

$$\begin{aligned} \bar{\mathcal{T}} &= \int_0^1 \frac{2(\varepsilon_0^2 - \Delta_0^2)d\alpha}{2\varepsilon_0^2 - \Delta_0^2 - \Delta_0^2 \cos\left[\frac{2(\varepsilon_0 - \Delta_0)mL}{\hbar^2 k_f} + 2\pi\alpha - \theta_0\right]} \\ &= \frac{2(\varepsilon_0^2 - \Delta_0^2)}{\sqrt{(2\varepsilon_0^2 - \Delta_0^2)^2 - \Delta_0^4}} = \frac{\sqrt{\varepsilon_0^2 - \Delta_0^2}}{\varepsilon_0}. \end{aligned} \quad (36)$$

Integrating over  $\alpha$  in the short oscillation period we ignored slow variation of the energy  $\varepsilon_0$  within the period.

#### IV. THE GROUND STATE (QUASIPARTICLE VACUUM)

##### A. Vacuum current

In the ground state in the superconducting layers the electron fluid is at rest, and there are no currents. Mathematically in our model the bound-state phase  $\theta_0$  is an independent parameter, and the energy of Andreev states depends on it. In order to determine the ground state, one should find the  $\theta_0$ -dependent energy of Andreev states and minimize it with respect to  $\theta_0$ . Since the charge current is determined by the derivative of the energy with respect to  $\theta_0$ , after minimization the current vanishes as it should be in the ground state.

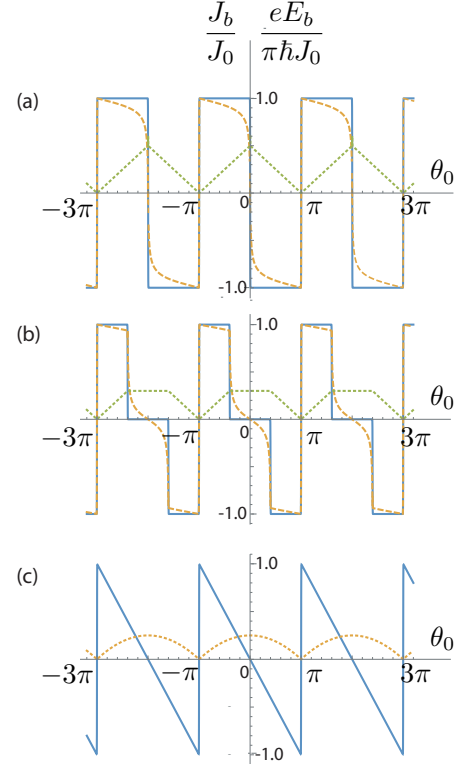


FIG. 2. The vacuum current and energy vs. the bound-state phase  $\theta_0$ . Currents calculated neglecting or taking into account penetration of Andreev states into superconducting layers at  $L/\zeta_0 = 50$  are shown by solid and dashed lines respectively. The vacuum energy as a function of the phase  $\theta_0$  is shown by dotted lines. The plots for  $\alpha$  and  $1 - \alpha$  are identical. (a)  $\alpha = 0$ . (b)  $\alpha = 0.2$ . (c) The current and the energy averaged over  $\alpha$ .

Neglecting the penetration depth  $\zeta$  in Eq. (30), the total current of all bound states vanishes if the numbers of states with positive and negative momenta [two signs in Eq. (30)] are equal, and they cancel one another. This is the case at phases  $\theta_0 = 0$  and  $\theta_0 = \pm\pi$ . However, at tuning the phase  $\theta_0$  energy levels move. At the both borders of the Andreev energy spectrum  $\varepsilon_0 = 0$  and  $\varepsilon_0 = \Delta_0$  new levels can enter the gap and others can exit from it. If  $\alpha = 1/2$  the entrance and the exit processes at the two borders are synchronized: at  $\theta_0 = \pm\pi$  a level exits (enters) at the lower border  $\varepsilon_0 = 0$  [see Eq. (26)] and simultaneously a level enters (exits) at the upper border  $\varepsilon_0 = \Delta_0$  [see Eq. (28)]. The numbers of states with positive and negative momenta remain equal, and the total current vanishes. At  $\alpha \neq 1/2$  levels enter or exit at the lower border of the Andreev spectrum at  $\theta_0 = \pm\pi$  as before, but levels cross the upper border at  $\theta_0 = \pm 2\pi\alpha$ . At  $-\pi < \theta_0 < -2\pi\alpha$  and  $\pi > \theta_0 > 2\pi\alpha$  there is one state with a positive or negative momentum without its counterpart with an opposite-sign momentum. This means that the total momentum is  $\pm\hbar k_f$  and the total

electric current is  $\pm ev_f/L$ . Eventually the total bound-state current is

$$J_b = \sum_s j(s) = J_0 \sum_s [2H(\theta - 2\pi s - \pi) - H(\theta - 2\pi s - \alpha) - H(\theta - 2\pi s - 2\pi + \alpha)], \quad (37)$$

where  $H(q)$  is the Heaviside step function and

$$J_0 = \frac{ev_f}{L} = \frac{\pi e \hbar n_0}{2mL}. \quad (38)$$

Deriving this formula we used the relation  $k_f = \pi n_0/2$  between  $k_f$  and the 1D electron density  $n_0$ . After this substitution the formula becomes valid also for 2D and 3D systems bearing in mind that at this generalization  $n_0$  and  $J_b$  become the electron density and current density in 2D and 3D systems respectively. The stepwise dependence of the current  $J_b$  on the phase  $\theta_0$  at various  $\alpha$  is shown in Figs. 2(a)–(b) by solid lines.

The phase-dependent energy

$$E_b(\theta_0) = \frac{\hbar}{2e} \int_{-\pi}^{\theta_0} J_b(\theta'_0) d\theta'_0 \quad (39)$$

is also shown in Fig. 2(a)–(c) by dotted lines. It is remarkable that the energy has a minimum not at zero phase, but at  $\theta_0 = \pm\pi$ . Thus, the ballistic SNS sandwich is a  $\pi$  Josephson junction. While in a usual Josephson junction the current is positive in the interval of the phase  $\theta_0$  from 0 to  $\pi$ , in a  $\pi$  junction the current is negative in this interval as in Figs. 2(a)–(b).

In our derivation of the vacuum current dependence on  $\theta_0$  we used the concept of the spectral flow, which is rather popular in the analysis of SNS junctions (see, e.g., Refs. 19 and 20). The concept assumes that tuning of the phase  $\theta_0$  leads to steady motion of Andreev levels, which cross the whole gap, i.e., enter the gap on one gap edge and exit from the gap on the other edge. However, this picture is valid only in the limit of infinite Fermi wave number when the Andreev level are degenerate at the phases 0 and  $\pi$ . Even small corrections to this limit lift this degeneracy introducing small gaps at the phases 0 and  $\pi$ . As a result, at phase tuning the Andreev levels do not cross the gap but oscillate within bands separated by the aforementioned small gaps. Our conclusion about the  $\pi$ -junction remains valid even after this modification of topology of Andreev levels. This is illustrated in Fig. 3 for the case  $\alpha = 0$  shown in Fig. 2(a). Figure 3 shows the variation of the Andreev-level energies with varying phase  $\theta_0$ . In shaded part of the spectrum at any phase the numbers of levels with positive and negative slope (i.e., with positive and negative currents) coincide. Thus,

these levels contribute nothing to the total vacuum current. The variation of the total vacuum current with the phase reduces to the contribution of the unshaded band closest to the gap edge. This contribution given by the canonical expression Eq. (30) coincides with that shown by a solid line in Fig. 2(a).

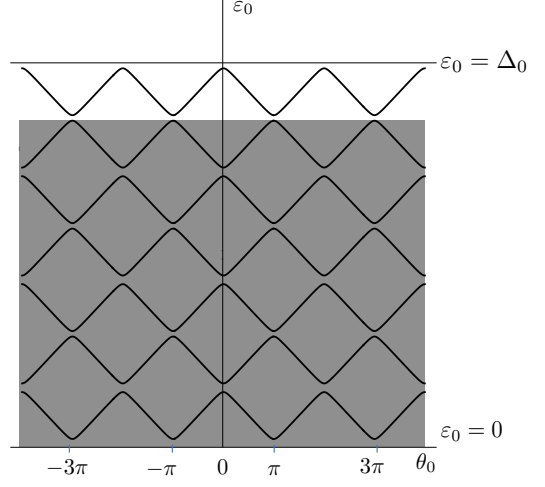


FIG. 3. The Andreev spectrum variation at tuning the bound-state phase  $\theta_0$ . In the shaded area the number of Andreev states with energies growing and decreasing with  $\theta_0$  are equal and the total current in these states vanishes (see the text). Only the unshaded band closest to the gap edge  $\varepsilon_0 = \Delta_0$  is responsible for the total current periodical dependence on  $\theta_0$ .

The periodic dependence of the current on the incommensurability parameter is fragile. In 2D and 3D systems integration over the transverse components of the wave vectors is expected to eliminate this dependence. It is reasonable to consider the current averaged over  $\alpha$  in the interval from 0 to 1. After averaging the current periodically depends only on the phase  $\theta_0$ . In the interval  $-\pi < \theta_0 < \pi$

$$J_b = -J_0 \frac{\theta_0}{\pi}. \quad (40)$$

The periodical saw-tooth dependence of the current on  $\theta_0$  is shown in Fig. 2(c).

However, the penetration depth  $\zeta$  diverges at  $\varepsilon_0 \rightarrow \Delta_0$ . According to Eq. (30), at  $\zeta \rightarrow \infty$  the current in the bound state crossing the upper gap border vanishes. Therefore, we performed a more accurate calculation in this limit. At  $\Delta_0 - \varepsilon_0 \ll \Delta_0$  the spectrum of bound state is described by Eq. (28), and the total current in all bound states is

$$J_b = \frac{J_0}{2} \left\{ \left[ 1 - \frac{1}{\sqrt{1 + \frac{\Delta_0 L}{\hbar v_f} (2\pi\alpha - \theta_0)}} \right] H(2\pi\alpha - \theta_0) - \left[ 1 - \frac{1}{\sqrt{1 + \frac{\Delta_0 L}{\hbar v_f} (2\pi\alpha + \theta_0)}} \right] H(2\pi\alpha + \theta_0) \right\}$$

$$+ \zeta \left( \frac{1}{2}, \frac{\hbar v_f}{2\pi\Delta_0 L} + 1 + \alpha - \frac{\theta_0}{2\pi} \right) - \zeta \left( \frac{1}{2}, \frac{\hbar v_f}{2\pi\Delta_0 L} + 1 + \alpha + \frac{\theta_0}{2\pi} \right) \} . \quad (41)$$

Here

$$\zeta(z, q) = \sum_{s=0}^{\infty} \frac{1}{(q+s)^z} \quad (42)$$

is Riemann's zeta function [21]. The series for Riemann's zeta function at  $z = 1/2$  diverges, but the series for a difference of zeta functions with different arguments  $q$  converges at large  $s$ , which, nevertheless, correspond to energies satisfying the condition  $\Delta_0 - \varepsilon_0 \ll \Delta_0$ . Therefore, one can use the infinite series with  $s \rightarrow \infty$ . The vacuum current  $J_b$  calculated taking into account penetration of Andreev states into superconducting layers at  $L/\zeta_0 = 50$  is shown in Fig. 2(a)–(b) by dashed lines. Summarizing, the divergence of the penetration depth at  $\varepsilon_0 \rightarrow \Delta_0$  transforms the current jump at crossing of the gap edge  $\varepsilon_0 = \Delta_0$  by the Andreev level into a smooth crossover. But the width of the crossover is small compared to the distance between levels abd can be ignored in the limit  $L \rightarrow \infty$ .

In general, the contribution of continuum states to the current also depends on the phase  $\theta_0$  since the scattering parameters depend on  $\theta_0$ . But according to Eq. (35), this contribution is a periodic function of  $2\pi\alpha - \theta_0$ , which vanishes after averaging over  $\alpha$ . Focusing on the approach based on this averaging we may neglect the contribution of continuum states to the vacuum current.

## B. Vacuum density

In the ballistic regime the boundary conditions on the interface affect the wave function in the whole bulk, but it is natural to expect that the average density in the vacuum in the ballistic and the diffusive regime do not differ and are fully determined by the volume of the Fermi sphere. This follows from the principle that although dissipative processes are necessary for relaxation to the ground state (vacuum), the final ground state itself is not determined by these processes. Nevertheless, it is useful to check this principle for the SNS sandwich, although this is a check of our analysis rather than of the principle itself.

In the superconducting layers at  $x < -L/2$  and  $x > L/2$  all states are delocalized and form the continuum. For the determination of the vacuum particle density one can replace in Eq. (14) summation by integration, and the total vacuum density for the both possible spin directions and all possible directions of incident quasiparticles and holes is

$$n_0 = \frac{1}{\pi} \int_{-\infty}^{\infty} |v|^2 dk = \frac{1}{\pi \hbar v_f} \int_{-\infty}^{\infty} |v|^2 d\xi, \quad (43)$$

where

$$|v|^2 = |v_0|^2 \left[ 1 + \frac{R(\theta_0) + \mathcal{T}(\theta_0) + R(-\theta_0) + \mathcal{T}(-\theta_0)}{2} \right] = 1 - \frac{\xi}{\varepsilon_0}. \quad (44)$$

The value of  $n_0$  coincides with the density  $n_0 = 2k_f/\pi$  in a uniform superconductor. So, scattering does not affect the average density  $n_0$  in the superconducting layers.

We start the estimation of the density in the normal layer  $-L/2 < x < L/2$  from the contribution of the Andreev bound states. Any bound state is a superposition of a particle state and of a hole state with equal probability 1/2. Thus, in the normal layer with thickness  $L \gg \zeta_0$  the contribution of Andreev states to the vacuum density is simply a half of the number of bound states per unit length:

$$n_{0b} = \frac{2k_f}{\pi} \frac{\Delta_0}{\varepsilon_f} = n_0 \frac{\Delta_0}{\varepsilon_f}. \quad (45)$$

The contribution of the continuum states in the normal layer is

$$n_{0c} = \frac{1}{\pi \hbar v_f} \int_{-\infty}^{\infty} |v|^2 \bar{\mathcal{T}} d\xi = n_0 \left( 1 - \frac{\Delta_0}{\varepsilon_f} \right). \quad (46)$$

The averaged transmission probability  $\bar{\mathcal{T}}$  is given by Eq. (36). Together with the contribution Eq. (45) the total density  $n_0 = n_{0b} + n_{0c}$  is the same as in uniform normal metals or superconductors with the Fermi energy  $\varepsilon_f$ .

## V. MOVING COOPER PAIR CONDENSATE

### A. Effect of the Cooper pair condensate motion on Andreev states (Doppler shift)

Let us consider the case of the moving Cooper pair condensate when in the superconducting layers there is an order parameter phase gradient  $\nabla\phi$ , which determines the superfluid velocity  $v_s$ :

$$v_s = \frac{\hbar}{2m} \nabla\phi. \quad (47)$$

We must solve the Bogolyubov–de Gennes equations Eq. (3) with the gap

$$\Delta = \begin{cases} \Delta_0 e^{i\theta_+ + i\nabla\phi x} & x > L/2 \\ 0 & -L/2 < x < L/2 \\ \Delta_0 e^{i\theta_- + i\nabla\phi x} & x < -L/2 \end{cases} . \quad (48)$$

The solution differs from the solution Eqs. (19)–(21) obtained for the resting condensate by the presence of the additional factors  $e^{imv_s x/\hbar}$  and  $e^{-imv_s x/\hbar}$  in the expressions for the components  $u$  and  $v$  respectively. These factors are cancel in the boundary conditions, and the expressions for  $\varepsilon_0$  [Eqs. (25), (26) and (28)] and for the reflection and transmission probabilities [Eqs. (33)–(35)] remains valid. However, the energy  $\varepsilon$  of an Andreev state differs from  $\varepsilon_0$  by the Doppler shift:

$$\varepsilon(s, \pm\theta_0) = \varepsilon_0(s, \pm\theta_0) \pm v_s k_f. \quad (49)$$

In particular, at low energies  $\varepsilon_0 \ll \Delta_0$

$$\varepsilon(s, \pm\theta_0) = \frac{\hbar v_f}{2L} \left[ 2\pi \left( s + \frac{1}{2} \right) \pm (\theta_0 + \theta_s) \right], \quad (50)$$

where

$$\theta_s = \frac{2mLv_s}{\hbar} \quad (51)$$

is the phase difference across the normal layer as if it were not normal but superconducting (Fig. 1). Therefore, further it will be called superfluid phase.

According to Eq. (50), the effects of the bound-state phase  $\theta_0$  and the superfluid phase  $\theta_s$  on the energy are additive, and the energy depends only on their sum. But it is true as far as  $\theta_s$  (velocity  $v_s$ ) is small. In general, there is an essential difference between effects of  $\theta_0$  and  $\theta_s$  on the Andreev spectrum. We saw that variation of  $\theta_0$  makes the Andreev levels to move with respect to the Andreev spectrum borders. As a result, some new levels can emerge and some old ones can disappear. In contrast, variation of  $\theta_s$  leads to the shift of the Andreev spectrum as a whole without changing positions of levels with respect to the Andreev spectrum borders. This is illustrated in Fig. 4. The principle of the BCS theory that only solutions with positive energies should be taking into account refers to the energy  $\varepsilon_0$ , while the Doppler-shifted energy  $\varepsilon$  can be both positive or negative. If  $\varepsilon$  is negative the level is fully occupied at zero temperature. This is important for the further analysis.

## B. Charge currents due to the motion of the Cooper pair condensate

The expression for the charge current  $J_s$  produced by the moving Cooper pair condensate follows from Eq. (15), in which only the vacuum contribution is taken into account:

$$J_s = \frac{ie\hbar}{m} \sum_i (v_i^* \nabla v_i - v_i \nabla v_i^*), \quad (52)$$

where summation includes summation over bound states and over the continuum, the later one reduced to an integral. Comparing this expression with the vacuum contribution to the electron density in Eq. (14) one obtains that in all layers of the sandwich [3]

$$J_s = en_0 v_s, \quad (53)$$

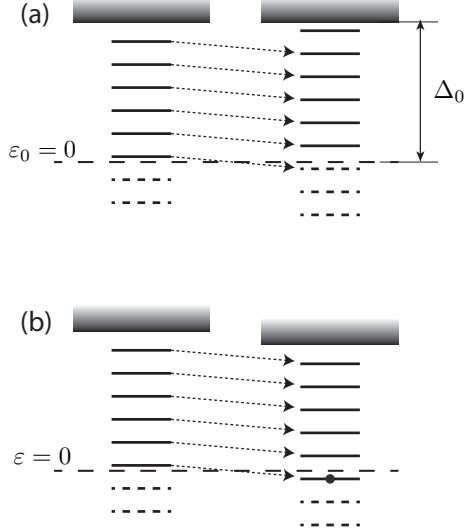


FIG. 4. Tuning of the energies of the Andreev states by the phases  $\theta_0$  and  $\theta_s$ . Horizontal solid lines show unoccupied Andreev levels. A horizontal solid line with a black circle shows an occupied Andreev level. Horizontal dashed lines show ghost levels with negative  $\varepsilon_0$ , which correspond to mathematically correct solutions of the Bogolyubov–de Gennes equations, but are not considered in the BCS theory as physically real bound states. Arrowed dashed lines show shifts of levels by tuning the phases  $\theta_0$  and  $\theta_s$ . (a) Tuning by the phase  $\theta_0$  at constant  $\theta_s$ . The lowest physical level crosses the energy  $\varepsilon_0 = 0$  and transforms to a ghost level, i.e., disappears. (b) Tuning by the phase  $\theta_s$  at constant  $\theta_0$ . All levels move together with the gap edge with the energy  $\varepsilon_0$  remained constant. The lowest physical level crosses the energy  $\varepsilon = 0$  and becomes occupied even at zero temperature.

as in a uniform superconductor. It is interesting that the expression is valid even for the case of full reflection of electrons from the superconductor boundary when the charge transport is impossible. This is a consequence of the absence of the charge conservation law in our model using the effective Hamiltonian Eq. (1) with broken gauge invariance. As will be explained in the beginning of Sec. VII, although solutions violating the charge conservation law are mathematically legitimate in the model, they should be ignored in the physical analysis.

## VI. QUASIPARTICLE CONTRIBUTION TO THE CURRENT

Andreev levels in the SNS sandwich are occupied at finite temperatures or even at zero temperature if the energy  $\varepsilon$  of some Andreev levels becomes negative due to the Doppler shift. We consider temperatures much lower than the gap  $\Delta_0$ . So quasiparticles in the superconducting layers are absent. But the temperature can be on the order or higher than the energy distance between Andreev levels. The contribution of quasiparticles

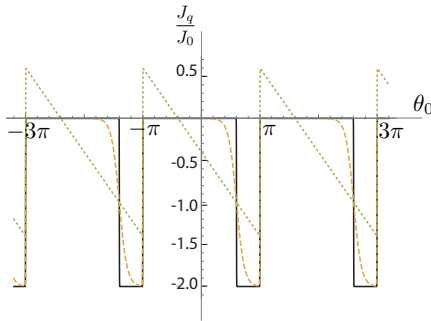


FIG. 5. The quasiparticle current vs. the bound-state phase  $\theta_0$  at  $\theta_s = 0.4\pi$ . Solid, dashed, and dotted lines show the current at zero temperature ( $\beta \rightarrow \infty$ ), low temperature ( $\beta = 30$ ), and high temperature ( $\beta \rightarrow 0$ ) respectively.

occupying Andreev levels at the temperature  $T$  is

$$J_q = 2J_0 \sum_s \left[ \frac{H(s + 1/2 + \theta_0/2\pi)}{e^{\beta(s+1/2+\theta_0/2\pi)} + 1} - \frac{H(s + 1/2 - \theta_0/2\pi)}{e^{\beta(s+1/2-\theta_0/2\pi)} + 1} \right], \quad (54)$$

where  $\theta = \theta_s + \theta_0$  and

$$\beta = \frac{\pi \hbar v_f}{LT}. \quad (55)$$

The Heaviside functions in numerators provide that only states of the Andreev spectrum with  $\varepsilon_0 > 0$  contribute to the current. At zero temperature ( $\beta \rightarrow \infty$ ) the Fermi distribution function also becomes the Heaviside function, and the quasiparticle current is

$$J_q = -\frac{\theta_s}{|\theta_s|} 2J_0 \quad (56)$$

in the interval

$$2\pi \left( s + \frac{1}{2} \right) - \theta_s < \theta_0 < 2\pi \left( s + \frac{1}{2} \right). \quad (57)$$

At high temperatures ( $\beta \rightarrow 0$ ) the summation in Eq. (54) can be replaced by integration. In the interval  $|\theta_s|, |\theta_0| < 2\pi$ :

$$J_q \approx 2J_0 \sum_s \left[ \frac{H(s + 1/2 + \theta_0/2\pi)}{2 + \beta(s + 1/2 + \theta_0/2\pi)} - \frac{H(s + 1/2 - \theta_0/2\pi)}{2 + \beta(s + 1/2 - \theta_0/2\pi)} \right] \approx -2J_0 \frac{\theta}{\pi} \int_0^\infty \frac{\beta ds}{(2 + \beta s)^2 - \beta^2 \theta^2 / 4\pi^2} = -J_0 \frac{\theta}{\pi}. \quad (58)$$

The contribution of quasiparticles at occupied Andreev states to the current is shown in Fig. 5 for  $\beta \rightarrow \infty$  (zero temperature),  $\beta = 30$  (low temperature), and  $\beta \rightarrow 0$  (high temperature) by the solid, dashed, and dotted line respectively.

## VII. CHARGE CONSERVATION LAW AND CURRENT-PHASE RELATION

As already mentioned, our model does not satisfy the charge conservation law, and solutions of the model, in which a current in any layer is independent from currents in other layers, are mathematically correct. However, only those solutions, which *do satisfy* the charge conservation law, have a physical meaning and must be chosen. One can meet this requirement by imposing the condition that in the stationary case currents in the normal layer do not differ from currents in the superconducting layers. Since the motion of the condensate with the velocity  $v_s$  produces the same current in all layers, the vacuum and quasiparticle currents in Andreev states must cancel one another. This yields the current–vacuum phase relation shown in Fig. 6 for zero and high temperature. We neglected small corrections to the vacuum current due to penetration of Andreev states into superconducting layers.

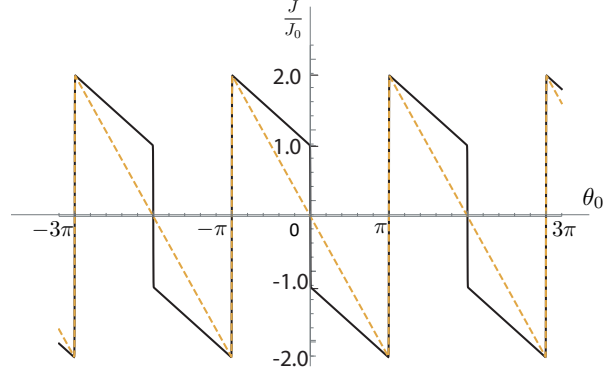


FIG. 6. The current–phase  $\theta_0$  relation for zero (solid line) and high (dashed line) temperature.

However, the bound-state phase  $\theta_0$  is not a phase, which must be used in the canonical description of the Josephson junction by the pair of conjugate variables “charge–phase”. The proper phase is the total phase difference across the normal layer  $\theta = \theta_0 + \theta_s$ , which we shall call Josephson phase (Fig. 1). The time derivative of the phase  $\theta$  determines the voltage drop across the normal

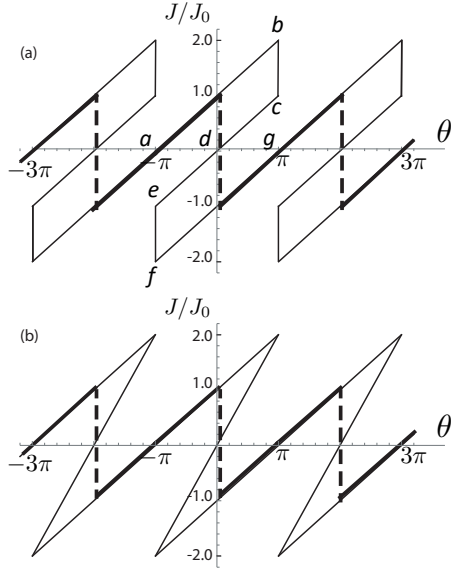


FIG. 7. The current–phase  $\theta$  relation. (a) Zero temperature. (b) High temperature. The thick solid and dashed line shows the adiabatic current–phase relation at extremely small voltage bias.

layer:

$$V = \frac{\hbar}{2e} \frac{d\theta}{dt}. \quad (59)$$

The current–phase relation for the Josephson phase  $\theta$  is shown for zero temperature in Fig. 7(a) and for high temperature in Fig. 7(b). The relation is quite bizarre: it is not single-valued at fixed phase  $\theta$ .

Let us discuss branches of the current–phase  $\theta$  curve in the interval  $(-\pi, \pi)$  at zero temperature shown in Fig. 7(a). At the branch  $cde$  the linear growth of the current with phase  $\theta$  is connected with linear growth of  $\theta_s$  at constant  $\theta_0 = 0$ . It will be called 0-branch. At the branches  $ab$  and  $fg$  the current grows linearly with  $\theta$  at constant  $\theta_0 = -\pi$  and  $\theta_0 = \pi$  respectively. They will be called  $\pi$ -branches. Along the vertical branches  $bc$  and  $ef$  the Josephson phase  $\theta = \theta_0 + \theta_s$  does not vary while the phase  $\theta_0$  varies between 0 and  $\pm\pi$ . It is necessary to stress that the incommensurability parameter  $\alpha$  determines the dependence of the current on the phase along the vertical branch, but does not affect the branch itself. Thus the procedure of averaging over  $\alpha$  does not affect the current–phase curve either. Along the vertical branches with  $\theta = \pm\pi$  the lowest Andreev level has zero energy, and the current variation is due to variation of the occupation of this level between 0 and 1. At high temperatures [Fig. 7(b)] the  $\pi$ -branches do not differ from those at zero temperature. Along the 0-branch the bound-state phase  $\theta_0$  is not constant, but the branch still crosses the abscissa axis at  $\theta_0 = 0$ .

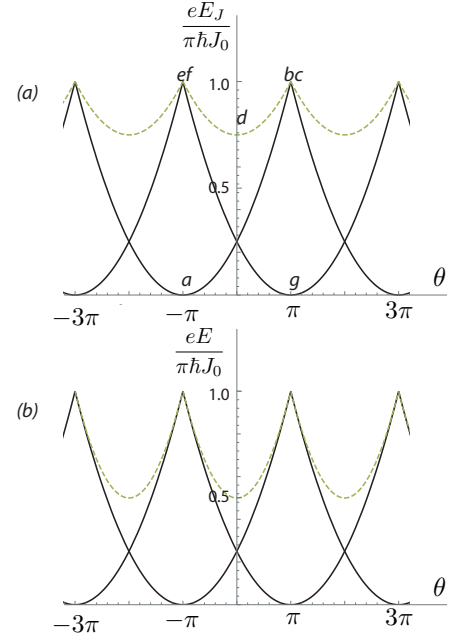


FIG. 8. The Josephson energy vs. Josephson phase  $\theta$ . Solid lines show  $\pi$ -branches, and dashed lines show 0-branches. (a) Zero temperature. The path  $a b c d e f g$  on this plot is mapping of the same path on the current–phase plot in Fig. 7(a). (b) High temperature.

The Josephson current satisfies the canonical relation

$$J = \frac{2e}{\hbar} \frac{\partial E_J}{\partial \theta}. \quad (60)$$

The Josephson energy  $E_J$  vs. the Josephson phase  $\theta$  is plotted in Fig. 8 for zero and high temperatures. There are only two branches on these plots:  $\pi$ -branches (solid lines) and 0-branches (dashed lines). The vertical branches  $bc$  and  $ef$  on the current–phase curve reduce to points since the energy does not vary along them.

Further we shall discuss possible behavior of the SNS sandwich in various cases.

#### A. Adiabatic current–phase relation at weak voltage bias

We start from the case of extremely weak constant voltage bias, which leads to adiabatic tuning of the phase  $\theta$  starting from the ground state at  $\theta = -\pi$  or  $\theta = \pi$ . The current grows until the phase  $\theta$  reaches the value 0 or  $2\pi$ . In principle, the current may continue to grow further, but at  $\theta > 0$  and at  $\theta > 2\pi$  the lower  $\pi$ -branch of the current–phase curve has a lower energy, and in a truly adiabatic process the jump from the upper  $\pi$ -branch to the lower one is expected. In Fig. 7 the expected adiabatic current–phase curves are shown by thick solid and dashed lines at zero and high temperature.

The adiabatic current–phase curve reminds the curve obtained by Bardeen and Johnson [3] at zero temperature with the same critical current

$$J_{cV} = J_0 = ev_f/L, \quad (61)$$

although differs from the latter by the shift  $\pi$  along the abscissa axis  $\theta$ .

Our analysis does not confirm the conclusion of previous works [3] that the temperature of the order of the energy interlevel distance strongly suppresses the supercurrent. The reason for disagreement is the following. Bardeen and Johnson [3] ignored the vacuum current determined by the phase  $\theta_0$  and considered only the 0-branch of the current–phase relation. In this case the quasiparticle current given by Eq. (58) differs only by sign but not in amplitude from the superfluid current, which in terms of the superfluid phase  $\theta_s$  is

$$J_s = en_0 v_s = J_0 \frac{\theta_s}{\pi}. \quad (62)$$

Thus, the two currents cancel one another apart from small corrections of the next order in  $1/L$ . However, the charge conservation law is satisfied only if one takes into account the  $\theta_0$ -dependent vacuum current, which cancels the quasiparticle current. Then the total currents at zero and high temperature do not differ.

### B. The stationary and nonstationary Josephson effect at current bias

At current bias of the SNS sandwich the critical current  $J_{cI} = 2J_0$  is two times larger than the critical current at weak voltage bias. If the current bias  $I$  is smaller than  $J_{cI}$  there is a stationary state with constant supercurrent  $I$  (the stationary Josephson effect). However, if  $I > J_{cI}$  only time-dependent solutions are possible, and the electron transport is accompanied by dissipation (the nonstationary Josephson effect).

Let us consider the SNS sandwich shunted by ohmic resistance  $R$  at the current bias  $I$  exceeding the critical one. The general expression for the average voltage for the overdamped Josephson junction is [16]

$$\bar{V} = \frac{2\pi R}{\int_{-\pi}^{\pi} \frac{d\theta}{I-J(\theta)}}, \quad (63)$$

where the integral in the denominator is taken over all branches of the original phase-dependent current (solid lines in Fig. 7) without jumps between branches. This yields the  $VI$  curve

$$\bar{V} = \frac{RJ_{cI}}{\ln \frac{(I+J_{cI})(I-J_{cI}/2)}{(I-J_{cI})(I+J_{cI}/2)}} \quad (64)$$

for zero temperature and

$$\bar{V} = \frac{2RJ_{cI}}{\ln \frac{I+J_{cI}}{I-J_{cI}}} \quad (65)$$

for high temperature. The curves transform to the Ohm law  $\bar{V} = RI$  at  $I \gg J_{cI}$ . They differ from the curve  $\bar{V} = R\sqrt{I^2 - J_{cI}^2}$  for the Josephson junction with the sinusoidal current–phase relation [16].

### C. The Josephson plasma mode. Is the SNS sandwich a weak link?

Although the dynamical analysis is beyond the scope of the present work, we still want to address the first elementary step of this analysis: the small oscillation around the ground state. For the Josephson junction this is the Josephson plasma oscillation. For an arbitrary current–phase relation the Josephson plasma frequency is given by

$$\omega_J = \sqrt{\frac{2e}{C\hbar} \frac{dJ(\theta)}{d\theta}}, \quad (66)$$

where  $C$  is the capacity per unit area of the planar Josephson junction and the derivative  $dJ(\theta)/d\theta$  is taken at  $\theta$ , which corresponds to the ground state. In usual Josephson junctions the Josephson plasma frequency is much lower than the plasma frequency

$$\omega_0 = \sqrt{\frac{4\pi e^2 n_0}{m}} \quad (67)$$

in the bulk superconductor. This inequality is in fact a necessary condition for the existence of the Josephson plasma mode localized at the Josephson junction and decaying inside the superconducting bulk. For the SNS sandwich  $\theta = \pm\pi$ ,  $C = 4\pi/L$ , and  $dJ(\theta)/d\theta = e\hbar n_0/2mL$ . Then  $\omega_J$  and  $\omega_0$  coincide. Thus, there is no localized Josephson plasma mode in the SNS sandwich. Swihart waves connected with the Josephson plasma mode are also impossible. The bulk plasma frequency  $\omega_0$  does not depend on whether a conductor is normal or a superconductor. It depends only on the electron density, which is the same in normal and superconducting layers.

The localized Josephson plasma mode in a usual planar Josephson junction exists because the junction is a weak link. The hallmark of weak link is that the supercurrent through the junction requires a much larger average gradient (ratio of the phase difference across the junction to its length, which determines its capacitance) than the same current in the bulk superconductor. The SNS sandwich is not a weak link in this meaning. So, the Josephson physics may be relevant not only for weak links as was assumed in textbooks [16].

### VIII. EFFECTS OF MAGNETIC FIELD AND JOSEPHSON VORTICES

Another manifestation that the SNS sandwich is not a weak link is its response to a weak magnetic field (Meissner effect). In the case of a usual planar Josephson

junction the magnetic field penetrates along the junction plane on the Josephson penetration depth, which is much longer than the London penetration depth into the superconducting bulk. Since the SNS sandwich is not a weak link and the electron density in the normal layer does not differ from the density in superconducting layers the Josephson penetration depth does not differ from the London penetration depth.

Despite the SNS sandwich is not a weak link with respect to linear effects like the Josephson plasma oscillation or the Meissner effect, it is not the case for nonlinear effects like the transition to the mixed state at the first critical magnetic field. The first critical magnetic field is determined by the energy of the magnetic vortex localized near the normal layer (Josephson vortex). Let us consider the Josephson vortex for the case when the London penetration depth  $\lambda$  is much longer than the thickness  $L$ . So two inequalities are satisfied:  $\lambda \gg L \gg \zeta_0$ . The axis of the straight vortex is in the middle of the normal layer, and at distance  $r$  from the axis exceeding  $L$  the structure of the vortex does not differ essentially from the Abrikosov vortex in the superconductor bulk. The area  $r > L$  gives the logarithmic contribution to the vortex energy per vortex length:

$$E_v = \left( \frac{\Phi_0}{4\pi\lambda} \right)^2 \ln \frac{\lambda}{L}, \quad (68)$$

where  $\Phi_0 = hc/2e$  is the magnetic flux quantum. The area  $r < L$  adds a number of order unity to the large logarithm. The energy  $E_v$  is lower than the energy of the Abrikosov vortex with the coherence length  $\zeta_0$  replacing  $L$  as a lower cut-off of the logarithm [16]. If  $L \gg \lambda$  the vortex energy is even smaller since the large logarithm in Eq. (68) is replaced by a number of order unity. This means that Josephson vortices are pinned to the normal layer, where their energy is less than the energy of Abrikosov vortices in the superconducting layers. The vortex energy determines the first critical magnetic field:  $H_{c1} = 4\pi E_v/\Phi_0$ .

## IX. SUMMARY

Let us summarize the main conclusions of this work:

- The ballistic SNS junction is a  $\pi$  junction. In its ground state the Josephson phase is not zero but  $\pm\pi$ .
- There is no essential suppression of the supercurrent through the ballistic SNS junction at temperatures on the order or higher than the energy distance between Andreev levels, but lower than the superconducting gap.
- Although the ballistic SNS junction has some properties of the Josephson junction, it is not a weak link in a strict sense. Therefore, the weak magnetic field penetrates into the normal layer on the

same London penetration depth as into the superconducting layers. There is no Josephson plasma mode localized at the normal layer.

- The magnetic vortices in the ballistic SNS junction have an essentially different structure from usual Josephson vortices, but still have energy lower than the energy of the Abrikosov vortex in the bulk of the superconductor. Therefore, vortices are pinned to the normal layer, and the first critical magnetic field for them is lower than for the superconductor bulk.

The conclusions of previous investigations were revised on the basis of our approach, which properly satisfies requirements imposed by the charge conservation law.

The  $\pi$  shift of the current–phase curve of the ballistic SNS junction can be detected experimentally by the same methods, which were used for phase shifts in superconductors with unconventional pairing [22].

Through the whole paper the ballistic SNS sandwich was considered as a Josephson junction. However, the sandwich has some features essentially different from properties of usual Josephson junctions. In fact, it is possible to describe it not in terms of the Josephson physics. Due to multiple Andreev reflection the ballistic normal layer does not destroy the phase coherence and supports the supercurrent  $J_s = en_0v_s$  with the same superfluid velocity  $v_s$  as in the superconducting layers. The supercurrent is restricted by the Landau criterion that the velocity  $v_s$  does not exceed the Landau critical velocity

$$v_L = \frac{\varepsilon_0}{\hbar k_f} = \frac{\pi\hbar}{2mL}. \quad (69)$$

At this velocity the energy of a quasiparticle at the lowest Andreev level with a positive energy  $\varepsilon_0$  if the condensate is at rest, becomes negative due to the Doppler shift. This yields the critical current  $J_{cV}$  given by Eq. (61). Since the Landau critical velocity inversely proportional to the layer thickness  $L$ , in the macroscopic (thermodynamic) limit  $L \rightarrow \infty$  the Landau critical velocity vanishes. Thus, “superconductivity” of the normal layer in the SNS sandwich is not a macroscopic, but a mesoscopic quantum phenomenon. It is similar to mesoscopic persistent currents in normal metal rings predicted theoretically [23] and observed experimentally (see Ref. 24 and references therein).

The model of the SNS junction without the proximity effect [1–3] used in our analysis is rather simplistic, but its analysis is an important first step for investigation of more complicated cases when normal and superconducting layers have different Fermi energies and effective masses, or the normal layer of the SNS sandwich is replaced by other materials, e.g., ballistic graphene or ballistic nanotubes. These cases are studied experimentally and theoretically nowadays [4–9]. Although the extension of the model on various cases of interest for nowadays experiments is needed, one may expect that

the conclusions about the  $\pi$  junction and the temperature dependence would survive this extension.

## ACKNOWLEDGMENTS

This work was started during my visit to the Low Temperature Laboratory of the Aalto University (Finland) in October 2019. I thank Dmitry Golubev and Pertti Hakonen for numerous discussions and comments, which stimulated my interest to this problem and helped its solution.

---

[1] I. O. Kulik, Macroscopic quantization and the proximity effect in SNS junctions, *Zh. Eksp. Teor. Fiz.* **57**, 1745 (1969), [*Sov. Phys.-JETP*, **30**, 944 (1970)].

[2] C. Ishii, Josephson currents through junctions with normal metal barriers, *Prog. Theor. Phys.* **44**, 1525 (1970).

[3] J. Bardeen and J. L. Johnson, Josephson current flow in pure superconducting–normal–superconducting junctions, *Phys. Rev. B* **5**, 72 (1972).

[4] D. Giuliano and I. Affleck, The Josephson current through a long quantum wire, *J. Stat. Mech.-Theory E* , P02034 (2013).

[5] X.-Z. Yan and C. S. Ting, Supercurrent transferring through  $c$ -axis cuprate Josephson junctions with thick normal-metal bridge, *J. Phys.: Condens. Matter* **21**, 035701 (2009).

[6] V. E. Calado, S. Goswami, G. Nanda, M. Diez, A. R. Akhmerov, K. Watanabe, T. Taniguchi, T. M. Klapwijk, and L. M. K. Vandersypen, Ballistic Josephson junctions in edge-contacted graphene, *Nat. Nanotechnol.* **10**, 761 (2015).

[7] M. Zhu, M. Ben Shalom, A. Mishchsenko, V. Fal’ko, K. Novoselov, and A. Geim, Supercurrent and multiple Andreev reflections in micrometer-long ballistic graphene Josephson junctions, *Nanoscale* **10**, 3020 (2018).

[8] S. Backens and A. Shnirman, Current–phase relation in a topological Josephson junction: Andreev bands vs. scattering states, arXiv:2010.03401.

[9] R. Delagrange, R. Weil, A. Kasumov, M. Ferrier, H. Bouchiat, and R. Deblock,  $0-\pi$  quantum transition in a carbon nanotube Josephson junction: Universal phase dependence and orbital degeneracy, *Phys. Rev. B* **93**, 195437 (2016).

[10] V. V. Ryazanov, V. A. Oboznov, A. Y. Rusanov, A. V. Veretennikov, A. A. Golubov, and J. Aarts, Coupling of two superconductors through a ferromagnet: Evidence for a  $\pi$  junction, *Phys. Rev. Lett.* **86**, 2427 (2001).

[11] R. R. Schulz, B. Chesca, B. Goetz, C. W. Schneider, A. Schmehl, H. Bielefeldt, H. Hilgenkamp, J. Mannhart, and C. C. Tsuei, Design and realization of an all  $d$ -wave dc  $\pi$ -superconducting quantum interference device, *Appl. Phys. Lett.* **76** (2000).

[12] J. A. van Dam, Y. V. Nazarov, E. P. A. M. Bakkers, S. D. Franceschi, and L. P. Kouwenhoven, Supercurrent reversal in quantum dots, *Nature* **442**, 667 (2006).

[13] A. F. Volkov, New phenomena in Josephson SINIS junctions, *Phys. Rev. Lett.* **74**, 4730 (1995).

[14] P. G. de Gennes, *Superconductivity of metals and alloys* (Benjamin, 1966).

[15] C. Virgilio Nino and R. Kuemmel, Quantum stability and screening in superconducting metallic weak links, *Phys. Rev. B* **29**, 3957 (1984).

[16] M. Tinkham, *Introduction to superconductivity*, 2nd ed. (McGraw-Hill, 1996).

[17] E. B. Sonin, Transverse force on a vortex and vortex mass: effects of free bulk and vortex-core bound quasi-particles, *Phys. Rev. B* **87**, 134515 (2013).

[18] E. B. Sonin, *Dynamics of quantised vortices in superfluids* (Cambridge University Press, 2016).

[19] Y. Makhlin and G. E. Volovik, Spectral flow in Josephson junctions and effective Magnus force, *Pis’ma Zh. Eksp. Teor. Fiz.* **62**, 923 (1995), [*JETP Lett.* **62**, 941–946 (1995)].

[20] M. Stone, Spectral flow, Magnus force, and mutual friction via the geometric optics limit of Andreev reflection, *Phys. Rev. B* **54**, 13222 (1996).

[21] I. S. Gradshteyn and I. M. Ryzhik, *Table of integrals, series, and products*, seventh ed. (Academic Press, 2007).

[22] D. J. Van Harlingen, Phase-sensitive tests of the symmetry of the pairing state in the high-temperature superconductors—Evidence for  $d_{x^2-y^2}$  symmetry, *Rev. Mod. Phys.* **67**, 515 (1995).

[23] M. Büttiker, Y. Imry, and R. Landauer, Josephson behavior in small normal one-dimensional rings, *Physics Letters A* **96**, 365 (1983).

[24] H. Bluhm, N. C. Koshnick, J. A. Bert, M. E. Huber, and K. A. Moler, Persistent currents in normal metal rings, *Phys. Rev. Lett.* **102**, 136802 (2009).